

## CHAPTER ONE HUNDRED NINETY ONE

### Hydrodynamic Forces on a Circular Cylinder due to Combined Wave and Current Loading

Yuichi Iwagaki\* and Toshiyuki Asano\*\*

#### ABSTRACT

The hydrodynamic force acting on a circular cylinder in a wave-current co-existing field and its generating mechanism are discussed. This study focuses on the asymmetries of both the water particle movement and the resultant vortex property with respect to the cylinder, which produce inherent characteristics in the hydrodynamic forces in the wave-current co-existing field.

First of all, the vortex property around a circular cylinder in the wave-adverse current co-existing field has been examined by flow visualization tests. It has been found that the vortex property depends on the flow characteristics around the trough phase when the wave-current composite velocity becomes maximum and can be represented with a newly proposed  $K.C.$  number for the co-existing field.

Secondly, the characteristics of the in-line force has been made clear by evaluating the drag coefficient and the mass coefficient in the expanded Morison's equation for the co-existing field. These coefficients can be well arranged by  $(K.C.)^{\frac{1}{2}}$ , which is one of the newly proposed  $K.C.$  numbers, and their characteristics coincide with the existing results in the wave only field. The in-line hydrodynamic force in the co-existing field can be explained sufficiently by considering the vortex property in the same manner as clarified in the wave only field.

Thirdly, the characteristics of the transverse force (lift force) are discussed in connection with the vortex properties. It has also been found that the fluctuating frequency of the lift force is synchronized with the loading wave frequency.

#### 1. Introduction

Evaluation of wave forces acting on a circular cylinder is one of the most important subjects in coastal and ocean engineering. Recently, Sarpkaya and Isaacson<sup>1)</sup> systematically assembled and organized comprehensive research efforts in this field, and they pointed out several problems which remain unsolved. The study on hydrodynamic forces

\* Professor, Dept. of Civil Eng., Kyoto University, M. of ASCE

\*\* Research Associate, Dept. of Civil Eng., Kyoto University  
Yoshida-honmachi, Sakyo-ku, Kyoto 606 Japan

in wave-current co-existing fields is one of such problems. However, researches on this subject are scarce and as yet there is not a sufficient understanding.

A quasi wave-current co-existing field can be easily obtained either by oscillating a cylinder in the in-line direction in a uniform flow, or by moving it at a constant speed in a harmonically oscillating flow. Verley and Moe<sup>1,2)</sup> examined the drag and the mass coefficients by using the former field, while Horikawa et al.<sup>2)</sup> treated them in the latter field. However, the existing studies have not sufficiently discussed the hydrodynamic forces based on the vortex properties around a cylinder.

As an essential difference of the generation mechanism of the hydrodynamic forces in the wave-current co-existing field from that in the wave-only field, this study focuses on the asymmetry of a water particle movement with respect to a cylinder.

In the wave-only field, the water particle moves almost symmetrically in both phases of wave crest and wave trough, while in the co-existing field it does asymmetrically due to a superimposed current. Consequently, the properties of the vortex formation, development and shedding become different from the wave-only field, and they produce inherent characteristics in the hydrodynamic forces.

From the above mentioned viewpoint, in this study first of all, flow visualization tests are performed in wave and adverse current co-existing fields to examine the vortex properties.

Secondly, the characteristics of the in-line force are made clear through the experimental data of the drag and the mass coefficients in the expanded Morison's equation to the co-existing field. Moreover, the generation mechanism of the in-line force associated with the vortex properties is discussed in detail.

Thirdly, the characteristics of the lift force are examined in regard to both the lift coefficients and the fluctuating frequencies. Further, "synchronization" between the lift force fluctuation and the loading wave frequency in the co-existing field is examined.

## 2. Vortex properties around a circular cylinder in co-existing fields

### (1) Flow visualization test

Experiments were carried out in a wave tank, 27m long, 0.5m wide and 0.7m high, in which a circulating flow can be generated by a power pump. The water depth was kept constant 30cm. The vertical circular cylinders used in this test were 30 mm and 60mm in diameter.

Test runs were conducted under conditions that the wave frequency  $f$  was 0.5Hz, the wave heights  $H$  were 1.1~3.9cm, the currents were in the opposite direction to the wave propagation and their velocities varied 0~13.9 cm/sec. The flow visualization around the cylinder was performed with aluminum powder, and photographs of fluid motion at the water surface were taken with a motor-drive camera at the speed of 3 frames per second.

## (2) Experimental results and discussion

To clarify the effect of the current on the vortex properties, the experiments were carried out under the condition that the wave height and period are almost constant, and only the current velocity is varied.

Fig.1 shows the results of experiments when the surface  $K.C.$  numbers  $K.C._s$  calculated from the water particle velocity of only the wave component, are approximately equal to 3 and only the current velocity is varied.

$K.C._s$  is defined as follows:

$$K.C._s = u_{ms} T / D \quad (1)$$

in which,  $u_{ms}$  is the velocity amplitude of wave component at the still water level,  $T$  the wave period and  $D$  the diameter of a cylinder.  $u_{ms}$  was calculated from the small amplitude wave theory. The subscript 's' denotes the value at the water surface.

$(K.C._s)_\dagger$  and  $(K.C._s)_\ddagger$  in Fig.1 are introduced as new  $K.C.$  numbers in the co-existing field. Their definition will be described later. In these numbers, the water particle velocity is represented by a composite velocity of the wave and current components at the trough phase. The direction of the wave propagation in Fig.1 is from left to right, and that of current is from right to left.

Fig.1(a), which is the case of the wave-only field, shows that a pair of symmetric vortices are generated and they are not shed from the cylinder. Fig.1(b) shows the case when a current of 6.3 cm/sec in velocity is superimposed on the waves. In this figure, it is observed that a pair of symmetric vortices are generated at the phase III, when the composite velocity becomes large, and they develop, decay and vanish as the phase proceeds. Fig.1(c) is the case when a faster current than in the case of (b) is superimposed, so that the movement of the water particles is uni-directional throughout all phases. It is observed that one vortex is generated in one wave period at one side, and in the following wave period one vortex is generated at the other side. As the current velocity still increases, a pair of asymmetric vortices are generated as shown in Fig.1(d).

From Fig.1 and other visualization tests, the following vortex properties were made clear.

The vortices which are generated at the trough phase when the composite velocity becomes maximum dominate the vortex pattern all over the wave phases. The relation between the vortex pattern and  $(K.C._s)_\dagger$  or  $(K.C._s)_\ddagger$  coincides with that of existing results in the wave-only field.<sup>9), 10)</sup> It cannot be decided here which  $K.C.$  number best represents the vortex properties in the co-existing field, since the number of the experimental data is not sufficiently large. However, concerning the coefficients of the hydrodynamic force,  $(K.C._s)_\ddagger$  was found to be the better parameter to describe them than  $(K.C._s)_\dagger$ .

Meanwhile, the flow properties during the crest phase are so affected by the still existing vortices generated during the trough phase that the vortex properties cannot be explained by the

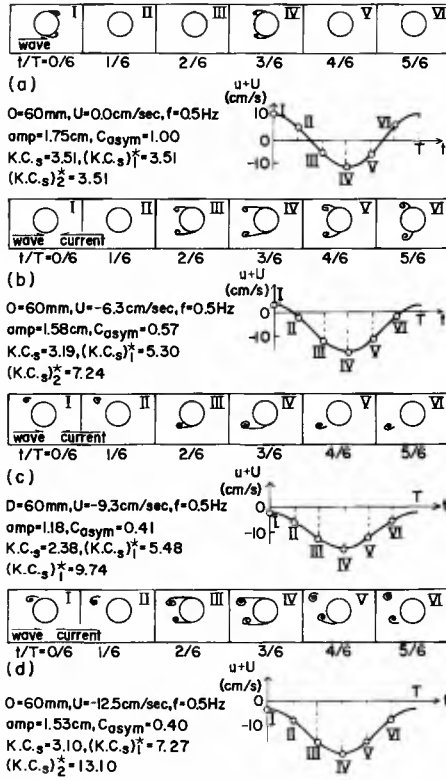


Fig.1 Changes of vortex pattern due to currents



Photo.1 An example of visual observations  
 (this photograph corresponds to Fig.1(c),  $t/T=4/6$ )

characteristics of the water particle movement.

The vortex properties clarified here are considered to control not only the characteristics of the in-line force but also those of the lift force.

### 3. Characteristics of in-line force acting on a circular cylinder

#### (1) Experimental procedure

The experimental apparatus was almost same as that used in the flow visualization test. Two vertically supported circular cylinders having  $D=30\text{mm}$  and  $60\text{mm}$  diameters are mainly used in this experiment. Test runs using a cylinder of  $20\text{mm}$  in diameter were added in order to obtain large  $K.C.$  numbers.

The experiments were conducted under the conditions of the wave frequencies  $f=0.5\sim 1.6\text{Hz}$  and the wave heights  $H=0\sim 21.0\text{cm/sec}$ . The currents were opposite direction to the wave propagation and their velocities varied  $U=0\sim 27.1\text{cm/sec}$ . The total number of the test runs was 80 for the wave only field, and 104 for the co-existing field. The water depth was kept constant  $40\text{cm}$ . The hydrodynamic forces were detected as moments by two strain gauges.

#### (2) Procedure of analysis

The hydrodynamic forces acting on a cylinder are represented by the following Morison's equation taking into account the effect of currents:

$$dF(z) = \frac{\rho}{2} C_D (u(z) + U(z)) |u(z) + U(z)| Dz + \frac{\rho\pi}{4} C_M D^2 \frac{\partial u(z)}{\partial t} dz \quad (2)$$

in which,  $dF$  is the horizontal hydrodynamic force acting on a segment  $dz$ ,  $\rho$  the density of fluid and  $C_D$  and  $C_M$  the drag and the mass coefficients respectively.

The wave component in the water particle velocity  $u(z)$  was assumed to be expressed by the small amplitude wave theory. The current velocity  $U(z)$  was assumed to be uniform in depth.

In this study two estimation methods of  $C_D$  and  $C_M$  were used. The first one is that either  $C_D$  or  $C_M$  is calculated at the specific phase when the inertia force or the drag force becomes zero respectively. Although this method is simple for calculation, it has some defects. That is to say, the reliability for the calculated value decreases significantly under such a wave and current composing condition that the water particle velocity or acceleration becomes small. Furthermore, for the case when the current velocity is larger than the amplitude velocity of the wave component,  $C_M$  cannot be calculated since the composite velocity never becomes zero throughout the wave phases.

Therefore, this method is applicable only for estimating  $C_D$  at the trough phase when the composite velocity becomes maximum.  $C_D$  estimated by the above mentioned method is expressed as  $(C_D)_{tr}$ , in which the subscript 'tr' means the value at the trough phase.

The second method estimating  $C_D$  and  $C_M$  is that proposed by Reid.<sup>5)</sup> By this method, water particle velocity  $u$  and acceleration  $\dot{u}$  are calculated from the water surface deviation  $\eta$  by using a numerical filter, and  $C_D$  and  $C_M$  are estimated from the measured hydrodynamic force by using the least squares method. The frequency response functions on  $\eta \sim u$  and  $\eta \sim \dot{u}$  with consideration of a current should be used.

The hydrodynamic force coefficients estimated by the above method are denoted as  $(C_D)_{b.f.}$  and  $(C_M)_{b.f.}$ , in which the subscript 'b.f.' means the best fit value.

### (3) Predominant parameters for expressing hydrodynamic force coefficients

Existing studies have treated the  $K.C.$  number and the Reynolds number as the predominant parameters expressing the hydrodynamic force coefficients in the wave only field. However, in the range of the Reynolds number in this experiment was between  $2 \cdot 10^3 \sim 2 \cdot 10^4$  where Sarpkaya<sup>6)</sup> reported that the changes of  $C_D$  and  $C_M$  with the Reynolds number are not so much. Accordingly, this study focuses on only the  $K.C.$  number as the predominant parameter for the force coefficients.

In the present study, two definitions are proposed as new  $K.C.$  numbers in the co-existing field. As shown in Chapter 2, the vortex properties around a cylinder throughout the phases are dominated by the water particle motion around the trough phase when the composite velocity becomes maximum.

As the first  $K.C.$  number, considering the composite velocity at the trough phase, the following parameter is introduced:

$$(K.C.)_1^* = (u_m + |U|)T/D \quad (3)$$

The physical meaning of the  $K.C.$  number can be considered as the ratio of the moving distance of a water particle in the one side direction of the cylinder  $s$  to the cylinder diameter  $D$ .

$$K.C. = \pi s/D \quad (4)$$

The second  $K.C.$  number is defined by the following equation expanding the above mentioned idea to the co-existing field.

For  $U \leq u_m$

$$(K.C.)_2^* = 2\pi \int_{t^*}^{T/2} |U + u_m \cos \sigma t| dt/D \quad (5)$$

in which,  $t^*$  denotes the time when the composite velocity becomes zero;

$$t^* = \cos^{-1}(-U/u_m)/\sigma \quad (6)$$

For  $U > u_m$

$$(K.C.)_2^* = \pi UT/D \quad (7)$$

As an expression for the component ratio of the wave and the current, the following parameter is introduced:

$$C_{asym} = u_m / (u_m + |U|) \tag{8}$$

This ratio becomes 1 at the limit of wave-only and tends to 0 as the current component becomes large compared with the wave component. Since this parameter represents the degree of asymmetry of the flow with respect to the center of a cylinder, the subscript of 'asym' denotes the abbreviation of asymmetry. In Eqs.(3), (5), (6) and (8), the velocity amplitude of the wave component  $u_m$  is defined as the root mean square value in the range from the water surface to the bottom.

Next, the ratio of the drag force to the inertia force is discussed. The maximum values of the drag and inertia forces throughout the wave phases,  $dF_{D,max}^T$  and  $dF_{M,max}^T$  are expressed by,

$$dF_{D,max}^T = (1/2) \rho C_D D (u_m + |U|)^2 dz \tag{9}$$

$$dF_{M,max}^T = (1/2) \rho \pi^2 C_M D^2 (u_m/T) dz \tag{10}$$

Accordingly, the ratio of both forces is calculated as follows:

$$\frac{dF_{D,max}^T}{dF_{M,max}^T} = \frac{C_D}{C_M} \left( \frac{u_m T}{D} \right) / \pi^2 \left( \frac{u_m}{u_m + |U|} \right)^2 = \frac{C_D}{C_M} (K.C.) / (\pi^2 C_{asym}^2) \tag{11}$$

The condition that the drag force is just equal to the inertia force is examined by using Eq.(11) under the assumption that  $C_D=1$  and  $C_M=2$ , independently of  $K.C.$  and  $C_{asym}$ . The result is shown in Fig.2, in which the predominant region of the drag or the inertia force is illustrated.

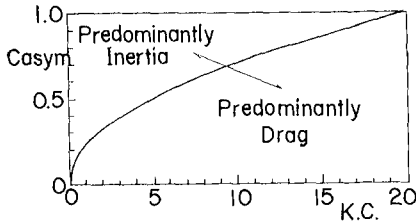


Fig.2 Predominant region of either drag or inertia force

(4) Experimental results and discussions

At first, preliminary experiments in the wave-only field were carried out. It is confirmed that the results coincide well with the existing ones in the wave-only field.

Next, the results obtained in the co-existing field are discussed. Fig.3 shows the relation between  $(C_D)_{tr}$  calculated at the wave trough phase and the  $K.C.$  number. It is observed that the characteristics of  $(C_D)_{tr}$  are not made clear by the  $K.C.$  number only, but they become evident after classifying the data into several ranges of  $C_{asym}$ . Also

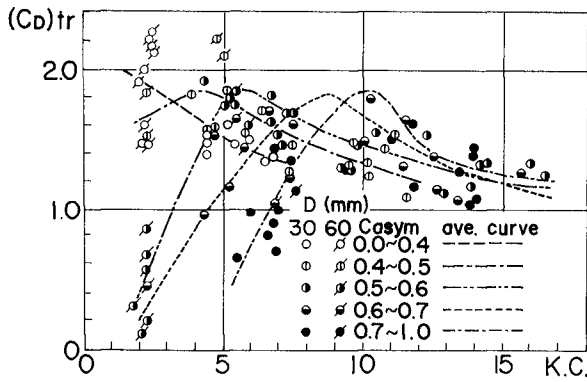


Fig.3 Drag coefficient  $(C_D)_{tr}$  at trough phase versus K.C. number (co-existing field)

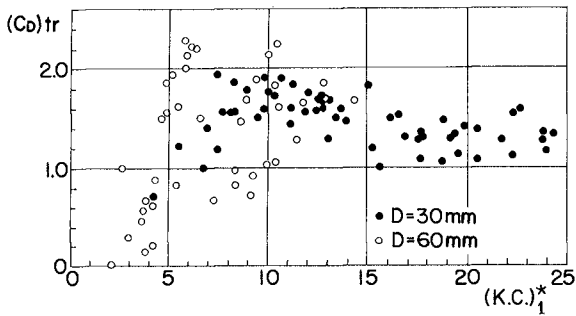


Fig.4 Drag coefficient  $(C_D)_{tr}$  at trough phase versus  $(K.C.)_1^*$  (co-existing field)

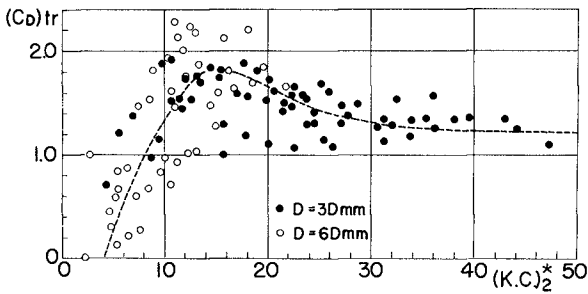


Fig.5 Drag coefficient  $(C_D)_{tr}$  at trough phase versus  $(K.C.)_2^*$  (co-existing field)

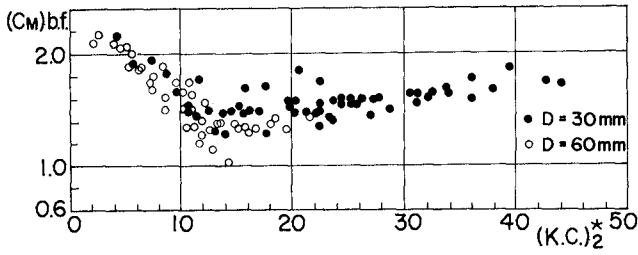


Fig.6 Mass coefficient  $(C_M)_{b.f.}$  fitting best with measured forces throughout wave phases versus  $(K.C.)^*_2$  (co-existing field)

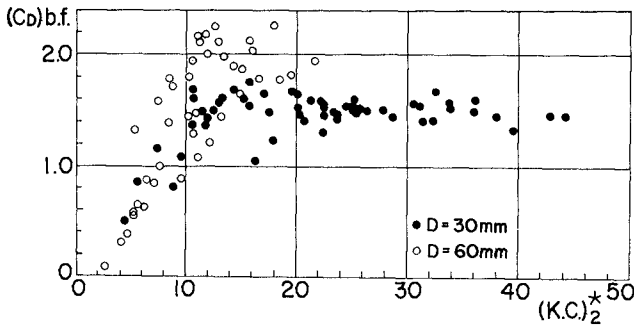


Fig.7 Drag coefficient  $(C_D)_{b.f.}$  fitting best with measured forces throughout wave phases versus  $(K.C.)^*_2$  (co-existing field)

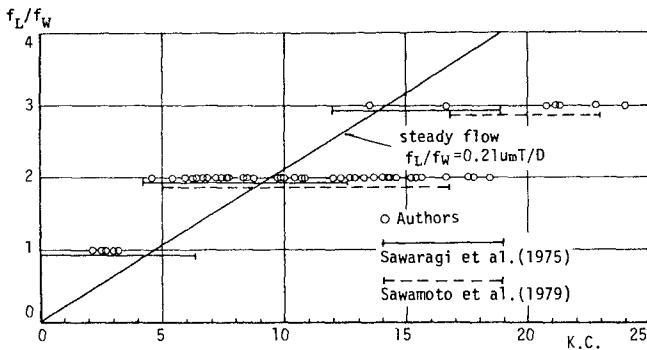


Fig.8 Ratio of lift force frequency  $f_L$  to loading wave frequency  $f_W$  versus  $K.C.$  (wave only field)

the peaks of the averaged curves shift in the direction of an increase in the  $K.C.$  number as  $Casym$  increases.

The results arranged by  $(K.C.)_1^*$  and  $(K.C.)_2^*$ , proposed as the new parameters in the co-existing field, are shown in Figs.4 and 5, respectively. In comparing both plots, the degree of scattering in Fig.5 using  $(K.C.)_2^*$  is less than that in Fig.4 using  $(K.C.)_1^*$ . In addition to this, from the view point of the physical meaning of the  $K.C.$  number, it is concluded that  $(K.C.)_2^*$  is a more appropriate parameter than  $(K.C.)_1^*$ .

The results of  $(C_D)_{b.f.}$  and  $(C_M)_{b.f.}$ , which are obtained by the least squares method in order to best fit the calculated values with the measured one, are discussed. Since  $(K.C.)_2^*$  is found to be the most suitable parameter as mentioned above, the data of  $(C_D)_{b.f.}$  and  $(C_M)_{b.f.}$  are also arranged by it. The results are shown in Figs.6 and 7 respectively.

Comparing Fig.5 with Fig.6, not much difference of the  $C_D$  values by the estimating methods is found. Furthermore, it is also made clear that the characteristics of the hydrodynamic force coefficients in the co-existing field show a good agreement with those in the wave-only field.

The reason why  $C_D$  and  $C_M$  are expressed well by  $(K.C.)_2^*$ , which represents the flow property around the trough phase, is considered that this flow property dominates the whole one throughout the wave phases. These characteristics of  $C_D$  and  $C_M$  can be explained by the established physical views in the wave only field<sup>4)</sup>.

Furthermore, several examinations on  $C_D$  and  $C_M$ , such as an effect of convective acceleration on them, were carried out and they were reported at the previous paper<sup>4)</sup>.

#### 4. Characteristics of lift force acting on a circular cylinder

##### (1) Experimental procedure

The experimental apparatus was almost same as that used in the flow visualization test and the in-line force measurements. Lift forces were measured by using two vertically supported cylinder of which diameters were 30mm and 60mm.

The experiments were conducted under the conditions of the wave frequency  $f=0.5\sim 0.8\text{Hz}$  and the velocities of adverse currents  $U=0\sim 25\text{cm/sec}$ . The water depth  $h$  was kept constant 40cm; however, several test runs were added under the condition of the water depth  $h$  reduced to 30cm to make current velocity large.

##### (2) Synchronization between lift force fluctuating frequency and loading wave frequency

Generation mechanism of lift force can be explained by vortex shedding around a cylinder. Accordingly, the vortex shedding frequency  $f_V$  generally coincides with the lift force fluctuating frequency  $f_L$ .

For a steady current, the relation between the current velocity  $U$  and the lift force fluctuating frequency  $f_C$  due to the current, which is

called here as Strouhal frequency, are described by Strouhal number  $S_t$ .

$$S_t = f_c D / U \quad (12)$$

The value of  $S_t$  is nearly constant at 0.2 in wide ranges of Reynolds number; therefore, the value of  $f_c$  increases continuously as the current velocity increases.

For the wave only field, however, it has been pointed out that  $f_L$  varies stepwisely with increasing in  $K.C.$ . Fig.8 shows the experimental results on the relation of  $f_L/f_W$  and  $K.C.$ . This result shows that even if the water particle velocity increases so far as the  $K.C.$  number does not exceed a certain value,  $f_L$  still remains constant. Namely, it is considered that the lift force fluctuation is strongly controlled by the loading wave frequency. This phenomenon is named here "synchronization".

The wave current co-existing field is considered as a transitional field connecting between the current only field and the wave only field; therefore, it is interesting to examine which property of currents or waves dominates in the co-existing field.

### (3) Experimental results on lift force fluctuation

Fig.9 shows some examples on the relation between lift force fluctuations and water surface deviations. Fig.9(a) is a result in the wave-only field, and shows that the frequency of the lift force is twice that of the wave. Fig.9(b) shows a result in the wave-current co-existing field. It is found in other many cases that  $f_L/f_W$  takes half odd numbers such as 0.5, 1.5, 2.5, ..., and this is considered to be an inherent property in the co-existing field.

Thus, in this study, the term of "synchronization" is used extensively for the case that  $2 \cdot f_L/f_W$  becomes an integer in addition to the case that  $f_L/f_W$  is an integer.

Fig.9(c) is a result of a relatively strong current and small waves combined loading. The figure shows that there is no obvious relation between the lift force fluctuations and the water surface deviations, and the value of  $f_L$  coincides with the Strouhal frequency  $f_c$  estimated from Eq.(12); therefore, it can be decided that the synchronization exists no longer in this case.

However, it is rather difficult to distinguish the case that  $f_L$  coincides with the Strouhal frequency  $f_c$  from the case that synchronization occurs, because when the value of  $f_L/f_W$  becomes larger than around 3, the lift force becomes irregular.

The experimental results on  $f_L/f_W$  are plotted in Fig.10. As the current velocity becomes large relative to the wave component, the value of  $f_L/f_W$  becomes large and finally  $f_L$  reaches to  $f_c$ . The data that  $f_L=f_c$  are plotted as a sign of "x" in the figure. In such cases that decision whether  $f_L$  is a multiple of  $f_W$  or equal to  $f_c$  is difficult, both signs are plotted in the figure.

It is noticeable in Fig.10 that  $2 \cdot f_L/f_W$  remains an integer even when the current velocity becomes large compared with the wave component

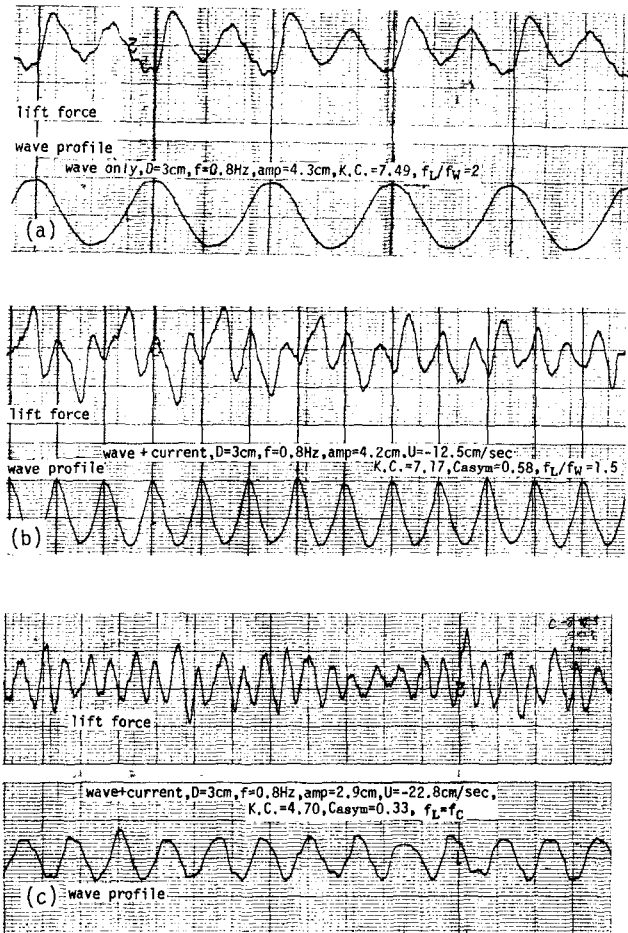


Fig.9 Records of lift force fluctuations and water surface deviations

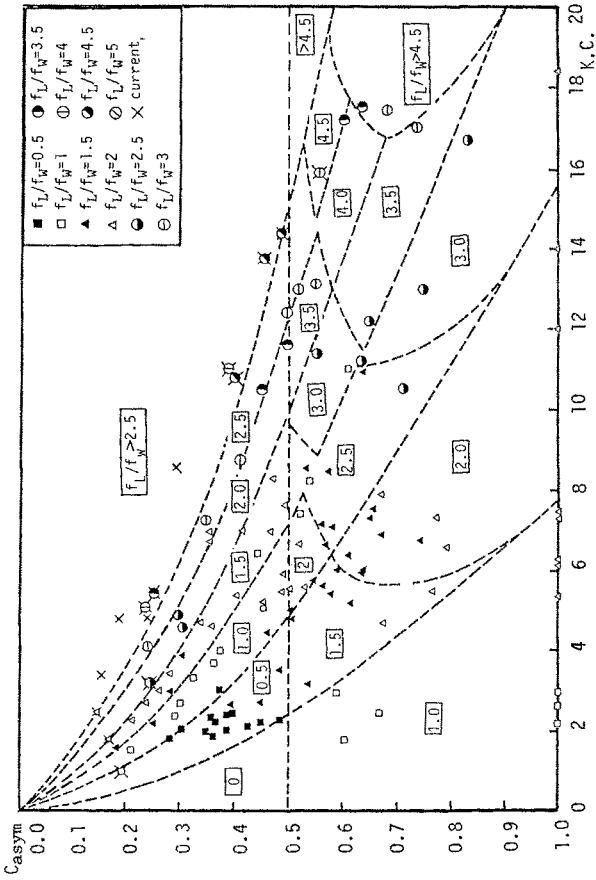


Fig.10 Comparisons of experimental results with calculated ones on a ratio of lift force frequency  $f_L$  to loading wave frequency  $f_W$

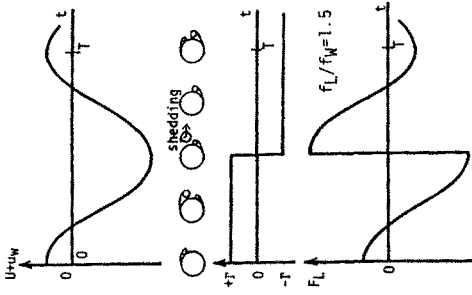


Fig.11 Schematic illustration of a model on  $f_L/f_W$

of water particle velocity.

It can be concluded that the lift force frequency or the vortex shedding frequency is strongly dominated by the loading wave frequency in the wave-current co-existing field.

This phenomenon is similar to the well known "synchronization" for a steady current field<sup>8)</sup>: When a cylinder is oscillated in a steady current, the forced oscillation locks the vortex-shedding frequency and controls the shedding process. Recently, a similar phenomenon is reported on aerodynamic responses on a bridge that a turbulent fluctuation of wind is possible to control the vortex-shedding<sup>9)</sup>.

#### (4) A model for predicting $f_L/f_W$

In this section, a simple model for predicting the experimental results on  $f_L/f_W$  is proposed.

Concerning an approximate estimation on the fluctuating frequency of lift force  $f_L$ , it is sufficient to consider only both properties of vortex shedding and mean flow velocity variation. It is not necessary to consider vortex generation, decay and movement.

Here, therefore, the lift force variations are approximated with the following Kutta-Joukowski type equation:

$$F_L = -\rho V \Gamma \quad (13)$$

in which  $\Gamma$  is a circulation around a cylinder.

Sawamoto and Kikuchi<sup>10)</sup> proposed a model to estimate lift forces in wave only field under the following assumptions: In a steady flow, a pair of vortices are shed from a cylinder when the moving distance of a water particle  $s$  exceeds 5 times the cylinder diameter  $D$ , which is easily obtained from the relationship of Eq.(12). They applied this idea extensively to the wave only fields, and estimated the number of shedding vortices during a wave period. Furthermore, they considered the variation of the circulation around a circular cylinder in the following way: Whenever a vortex sheds from a cylinder, the same magnitude and opposite sign circulation is added according to Kelvin's circulation theory.

Here, this study applied Sawamotos' idea to the wave-current coexisting field. Fig.11 shows schematically the variation of the circulation around a cylinder, the water particle velocity and the estimated lift force fluctuation.

In the wave only field, a water particle moves symmetrically with respect to the cylinder so far as non-linearity is ignored; therefore, equal number of vortices are shed from up-stream and down-stream sides of the cylinder. The number of shedding vortices while a water particle moves in one direction is presented by "n", then the total number of shedding vortices during a wave period is equal to  $2n$ . Consequently, the circulation  $\Gamma$  changes its sign  $2n$  times during a wave period. Meanwhile, the main stream velocity  $U+u_m \cos \omega t$  changes its sign 2 times during a wave period. Accordingly,  $f_L/f_W$  is given as

$$f_L/f_W = n + 1 \quad (14)$$

In the wave-current co-existing field, water particles move asymmetrically due to a superimposed current, so that the number of vortices from each side of the cylinder becomes different.

At first, we consider a case that current velocity  $U$  is smaller than the amplitude velocity of the wave component  $u_m$ . The numbers of shedding vortices from both sides of the cylinder are denoted as  $n_1$  and  $n_2$ . Since the circulation  $\Gamma$  changes its sign  $n_1 + n_2$  times and the main stream velocity does 2 times, the value of  $f_L/f_W$  for this case is calculated as follows:

For  $|U| \leq u_m$

$$f_L/f_W = (n_1 + n_2 + 2)/2 \quad (15)$$

Next, for another case of  $|U| \leq u_m$ , a water particle moves in the uni-direction throughout a wave period.  $\Gamma$  changes its sign  $n$  times, in which  $n$  denotes the number of shedding vortices during a wave period, while  $U + u_m \cos \omega t$  never changes its sign. Consequently, the following equation is obtained:

For  $|U| > u_m$

$$f_L/f_W = n/2 \quad (16)$$

It is easily confirmed from Eqs.(15) and (16) that  $f_L/f_W$  is possible to take a value of half odd number. The numbers of  $n_1$ ,  $n_2$ ,  $n$  are calculated based on the assumption that one vortex is shed when the moving distance  $s$  exceeds 2.5 times the cylinder diameter  $D$ . For example,  $n_1$  in Eq.(15) is calculated by following equation:

$$\begin{aligned} n_1 &= \left\{ 2 * \int_0^{t^*} (U + u_m \cos \omega t) dt / (2.5D) \right\} \\ &= \left\{ \frac{2}{5} \cdot \frac{K.C.}{\pi} \left( \sin \omega t^* + 2\pi \frac{U}{u_m} \frac{t^*}{T} \right) \right\} \end{aligned} \quad (17)$$

in which,  $\{ \}$  shows the maximum integer not to exceed the inside value of the bracket.  $t^*$  denotes the time when the wave-current component velocity becomes zero as shown in Eq.(6). If two parameters of  $K.C.$  (Eq.(1)) and  $C_{asym}$  (Eq.(8)) are given, all the values of  $n_1$ ,  $n_2$  and  $n$  can be calculated and then  $f_L/f_W$  also can be estimated from these values.

The results on  $f_L/f_W$  estimated by this model are shown in Fig.10 with the experimental results, where the boundaries on the values of  $f_L/f_W$  are drawn by dotted curves. The reason why the calculated  $f_L/f_W$  values vary at  $C_{asym}=0.5$  is that the model estimates them using the different equations between for  $|U| > u_m$  and for  $|U| \leq u_m$ .

From the comparison of calculated results with experimental ones, it is found that this simple model predicts satisfactorily well the experimental results including the property that  $f_L/f_W$  has a value of half odd number.

#### (5) Lift force coefficient in wave-current co-existing fields

In this section, the lift force coefficient and the predominant

parameters are discussed. The lift coefficient  $C_L$  in the co-existing field are defined as the following equation:

$$C_L = F_L / \{0.5\rho D(u_m + |U|)^2\} \quad (18)$$

in which,  $F_L$  is the individual peak value of the lift force fluctuation. Since lift forces generally do not show regular fluctuations even if regular forces load on a cylinder, it is necessary to use statistic representatives on  $C_L$ .

Here three representatives are used, such as, the mean, the one-third and the one-tenth largest lift coefficients which are denoted as  $\overline{C_L}$ ,  $C_{L1/3}$ , and  $C_{L1/10}$ , respectively.

In the wave only field, it has already been pointed out that  $C_L$  becomes the maximum when  $K.C.$  is around 10~12. Fig.12 shows the experimental results on the one-tenth largest lift force coefficient performed by the authors and Sawaragi-Nakamura<sup>9)</sup>.

Fig.13 shows the results on the mean lift coefficient  $\overline{C_L}$  in the wave-current co-existing field against  $K.C.$ . Since the parameter  $K.C.$  does not consider the current component, there appears much scatter.

Next, the same results are arranged by the newly proposed  $K.C.$  number in the co-existing field  $(K.C.)_{\frac{1}{2}}$  which is defined by Eqs. (5) and (7). The results are shown in Fig.14 and similar results on the one-third and the one-tenth largest lift coefficients  $C_{L1/3}$  and  $C_{L1/10}$  are shown in Figs.15 and 16 respectively.

It is found from these figures that the lift force co-efficients are well arranged by  $(K.C.)_{\frac{1}{2}}$  and take their maximum around  $(K.C.)_{\frac{1}{2}} = 10 \sim 12$ . This fact coincides with the property obtained in the wave only field as shown in Fig.12. The property that  $C_L$  takes the maximum around  $(K.C.)_{\frac{1}{2}} = 10 \sim 12$  is explained by the vortex property obtained in Chapter 2; that is, asymmetric vortices are generated in the flow condition when  $(K.C.)_{\frac{1}{2}} = 10 \sim 12$ .

It is concluded that  $(K.C.)_{\frac{1}{2}}$  which expresses the vortex property in the wave current co-existing field can represent the property of the lift force coefficient as well as the in-line force coefficients.

## 5. Conclusions

The vortex properties around a circular cylinder depend on the flow properties around the phase when the wave-current composite velocity is maximum.

The force coefficients for both in-line and transverse forces are arranged well by  $(K.C.)_{\frac{1}{2}}$  which is proposed as a new  $K.C.$  number in the wave-current co-existing field. The relations between these coefficients and  $(K.C.)_{\frac{1}{2}}$  are in good agreement with the results on the relations between the coefficients and  $K.C.$  established in the wave only field.

Furthermore, on the lift force frequency the following inherent properties in the co-existing field are obtained: the ratio of its

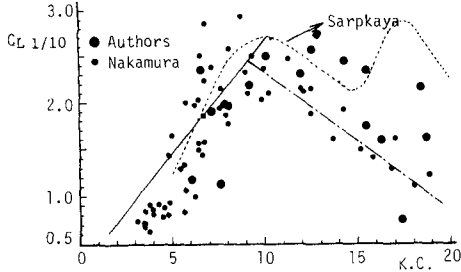


Fig. 12 One-tenth largest lift coefficient  $C_{L1/10}$  versus K.C. (wave only field)

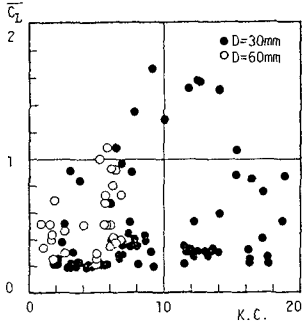


Fig. 13 Mean lift force coefficient  $\bar{C}_L$  versus K.C.

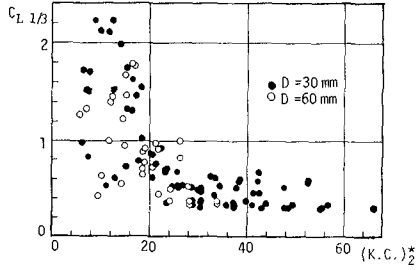


Fig. 15 One-third largest lift coefficient  $C_{L1/3}$  versus  $(K.C.)^2$

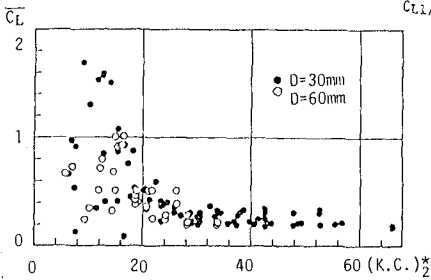


Fig. 14 Mean lift coefficient  $\bar{C}_L$  versus  $(K.C.)^2$

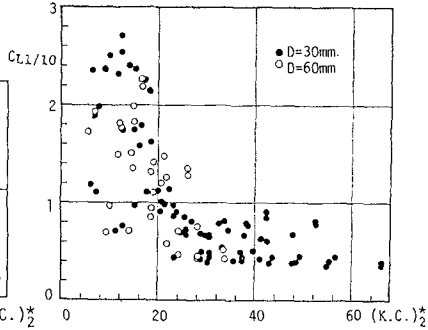


Fig. 16 One-tenth largest lift coefficient  $C_{L1/10}$  versus  $(K.C.)^2$

frequency to the loading wave frequency is possible to take a half odd numbers, and the both fluctuations synchronize each other.

#### Acknowledgement

This study is part of the research sponsored by the Grant-in-Aid for Scientific Research of the Ministry of Science, Culture and Education. The authors wish to express their appreciation to Messrs. F. Nagai and T. Yamada, former students at Department of Civil Engineering, Kyoto University, for their help in performing the experiments.

#### Reference

- 1) Bishop, R.E.D. and A.Y. Hassan : The lift and drag forces on a circular cylinder oscillating in a flowing fluid, Proc. Royal Soc. London, A277, pp.51-75, 1964.
- 2) Horikawa, K., M. Mizuguchi, O. Kitazawa and Y. Yanagimoto : On hydrodynamic force in wave-current field (part.1), Proc. 23th Conf. Coastal Eng. in Japan, pp.39-44, 1976 (in Japanese).
- 3) Iwagaki, Y. and H. Ishida : Flow separation, wake vortices and pressure distribution around a circular cylinder under oscillatory waves, Proc. 15th Coastal Eng. Conf., ASCE, pp.2341-2356, 1976.
- 4) Iwagaki Y., T. Asano and F. Nagai : Hydrodynamic forces on a circular cylinder placed in wave-current co-existing fields, Memoirs of Faculty of Eng., Kyoto Univ., Vol.45 No.1, pp.11-23, 1983.
- 5) Reid, R.O. : Correlation of water level variations with wave forces on a vertical pile for non-periodic waves, Proc. 6th Conf. Coastal Eng., pp.749-783, 1957.
- 6) Sarpkaya, T. : In-line and transverse forces on cylinders in oscillatory flow at high Reynolds number, Proc. of Offshore Technology Conference, Vol.2, pp.95-108, 1976.
- 7) Sarpkaya, T. and M. Isaacson : Mechanics of wave forces on offshore structures, Van Nostrand Reinhold Co., p.651, 1981.
- 8) Sawamoto, M. and K. Kikuchi : Lift forces on circular cylinder in an oscillating fluid, Proc. 26th Conf. Coastal Eng. in Japan, pp.429-433, 1979 (in Japanese).
- 9) Sawaragi T., T. Nakamura and H. Kita : Characteristics of lift forces on a circular pile in waves, Coastal Engineering in Japan, Vol.19, pp.59-71, 1976.
- 10) Sawaragi, T. and T. Nakamura : Analytical study of wave force on a cylinder in oscillatory flow, Coastal Structures 79, Vol.1, pp.154-173, 1979.
- 11) Shiraishi, N., M. Matsumoto and H. Okanan : Aeroelastic galloping of prismatic tower in the turbulent flow, Symposium on Wind Engineering, pp.273-279, 1982 (in Japanese).
- 12) Verley, R.L.P. and G. Moe : The forces on a cylinder oscillating in a current, The Norwegian Institute of Technology, Rep. No. STF60, A79061, p.58, 1979.